Activation Delay After Premature Stimulation in Chronically Diseased Human Myocardium Relates to the Architecture of Interstitial Fibrosis

Tokuhiro Kawara, MD; Richard Derksen, MD; Joris R. de Groot, MD; Ruben Coronel, PhD; Sara Tasseron, RT; André C. Linnenbank, PhD; Richard N.W. Hauer, MD; Hans Kirkels, MD; Michiel J. Janse, MD; Jacques M.T. de Bakker, PhD

Background—Progressive activation delay starting at long coupling intervals of premature stimuli has been shown to correlate with sudden cardiac death in patients with hypertrophic cardiomyopathy. The purpose of this study was to elucidate the mechanism of increased activation delay in chronically diseased myocardium.

Methods and Results—High-resolution unipolar mapping (105, 208, or 247 recording sites with interelectrode distances of 0.8, 0.5, or 0.3 mm, respectively) of epicardial electrical activity was carried out during premature stimulation in 11 explanted human hearts. The hearts came from patients who underwent heart transplantation and were in the end stage of heart failure (coronary artery disease, 4; hypertrophic cardiomyopathy, 1; and dilated cardiomyopathy, 6). Eight hearts were Langendorff-perfused. Epicardial sheets were taken from the remaining hearts and studied in a tissue bath. Activation maps and conduction curves were constructed and correlated with histology. Conduction curves revealing prominent increase of activation delay were associated with zones of dense, patchy fibrosis with long fibrotic strands. Dense, diffuse fibrosis with short fibrotic strands only marginally affected conduction curves. The course of conduction curves in patchy fibrotic areas greatly depended on the direction of propagation relative to fiber direction.

Conclusions—The study demonstrates that in chronically diseased human myocardium, nonuniform anisotropic characteristics imposed by long fibrotic strands cause a progressive increase of activation delay, starting at long coupling intervals of premature stimuli. The increase strongly depends on the direction of the wave front with respect to fiber direction and the architecture of fibrosis. **(*Circulation*. 2001;104:3069-3075.)**

Key Words: anisotropy ■ arrhythmia ■ collagen ■ conduction ■ mapping

Ventricular fibrillation is the main cause of sudden cardiac arrhythmic death and is often associated with structural heart disease.[1] Several risk stratification techniques have been developed to select patients prone to ventricular fibrillation.[2,3] Saumarez and coworkers[4] proposed that the electrophysiological substrate for ventricular arrhythmias can be identified in a particular patient by a pacing protocol using premature stimulation with a decremental sequence until the refractory period is reached. Their study showed that in patients with ventricular fibrillation and hypertrophic cardiomyopathy, the onset of activation delay started at long coupling intervals of the premature stimulus (early onset of activation delay) and that delay progressively increased on further shortening of these intervals. In controls and low-risk patients, activation delay characteristically remained constant and did not significantly increase until coupling intervals came close to the refractory period.[4]

The mechanism of early onset of activation delay after premature stimulation has not yet been determined in chronically diseased myocardium. During acute ischemia, early onset of activation delay seemed to be associated with delayed recovery of excitability and a reduced resting transmembrane potential.[5,6] Because ischemia is usually absent in chronically diseased myocardium, other factors must be responsible. It has been shown that discontinuities in myocardial bundles and wave front curvature around anatomical obstacles may result in activation delay.[7–10] We hypothesized that such abnormalities imposed by the altered myocardial architecture of chronically diseased myocardium may also lead to early onset of activation delay.

The objective of the present study was to clarify the mechanism of early onset of activation delay in chronically diseased myocardium. For this purpose, we correlated conduction properties during premature stimulation with the

Received August 17, 2001; revision received October 15, 2001; accepted October 15, 2001.

From the Experimental and Molecular Cardiology Group, Cardiovascular Research Institute, Amsterdam, and the Department of Medical Physics, Academic Medical Center, Amsterdam, the Netherlands (J.R.d.G., R.C., S.T., A.C.L., M.J.J.); the Heart Lung Center Utrecht, Utrecht, the Netherlands (R.D., R.N.W.H., H.K.); Biofunctional Informatics, School of Allied Health Sciences, Tokyo Medical and Dental University, Tokyo, Japan (T.K.); and the Interuniversity Cardiology Institute of the Netherlands, Utrecht, the Netherlands (J.M.T.d.B.).

Correspondence to Jacques M.T. de Bakker, PhD, Department of Experimental Cardiology, Meibergdreef 9, 1105AZ Amsterdam, the Netherlands. E-mail j.m.debakker@amc.uva.nl

histology of infarcted and cardiomyopathic hearts derived from patients undergoing heart transplantation in the end stage of heart failure.

Methods

Measurements were performed on 11 explanted human hearts (7 from women and 4 from men aged 39 to 63 years). Hearts came from patients who underwent heart transplantation during the end stage of heart failure. Four patients had coronary artery disease (with myocardial infarction), one suffered from hypertrophic cardiomyopathy, and 6 had dilated cardiomyopathy. Two patients were on amiodarone until surgery, and 2 others were on digoxin. Excised hearts were immersed in cold (4°C) Tyrode's solution. The aorta (n=3) or coronary arteries (n=5) of 8 hearts were cannulated and connected to a Langendorff-perfusion set up. Hearts were perfused (flow, 300 to 400 mL/min) with a mixture of human blood (50%) and Tyrode's solution. Epicardial ventricular sheets (5 by 5 cm, 1 mm thick) were taken from the remaining 3 hearts. These preparations were superfused in a tissue bath (epicardial surface up) with Tyrode's solution at 37±0.5°C. Superfusion diminishes the influence of the third dimension on propagation because only a thin layer (0.3 to 0. 5 mm) survives.

Recording Electrical Activity

High-resolution mapping of the electrical activity of ventricular epicardium was performed in both Langendorff-perfused hearts and superfused preparations. Recordings were made in unipolar mode. A single electrode attached to the aortic root (Langendorff-perfused hearts) or submerged in the tissue bath served as the reference electrode. Multiterminal plaque electrodes harbored 105, 208, or 247 terminals consisting of 70-μm diameter silver wires that were isolated except at the tip. Terminals were arranged in a 9×12, 16×13, or 19×13 matrix at interelectrode distances of 0.8, 0.5, and 0.3 mm, respectively. Plaque electrodes were positioned over nonfatty epicardial areas.

Programmed Stimulation and Data Acquisition

Electrical stimulation was applied with bipolar hook electrodes positioned adjacent to any one of the 4 sides of the multielectrode. Pacing was at twice diastolic current threshold with an 8-pulse drive train (cycle length, 600 ms) and 1 premature stimulus. Coupling intervals of premature stimuli were from 500 ms down to the refractory periods in steps of 10 ms. Electrograms were bandpass-filtered (0.5 Hz to 0.5 kHz), amplified 40 times, and digitized (16 bit resolution) at a sample rate of 1 kHz per channel.

Analysis of Electrograms

Electrograms were analyzed off-line with customized software. The point of steepest negative dV/dt in the electrogram was used as the local activation time. Activation maps were constructed from the local activation times, and conduction curves were obtained by plotting activation delay (interval between stimulus and activation time) against the coupling interval of the premature stimulus. To characterize conduction curves, we used the mean increase of delay (MID). This parameter was calculated by dividing the integrated increase of delay (gray area in Figure 1) by the interval between the basic cycle length (BCL) and the refractory period. For each position of the plaque electrode, MID was determined at all electrode terminals, allowing the construction of MID maps. The mean of the 105, 208, or 247 MID values (MID) was used as a measure of MID for the recording area.

Histology

Tissue at 16 of the 26 positions of the multielectrode in 8 hearts was subjected to histological investigation. Small pins were used to mark the corners of the recording electrode. Tissue at recording sites was excised and fixed in formalin. Sections with a thickness of 7 μm were made parallel to the epicardium, stained with picrosirius red, and examined by light microscopy for fibrosis. The amount of fibrosis in the recording area was determined using the KS 400 software package (Kontron) after digitizing sections with a slide scanner (Sprintscan 35, Polaroid).

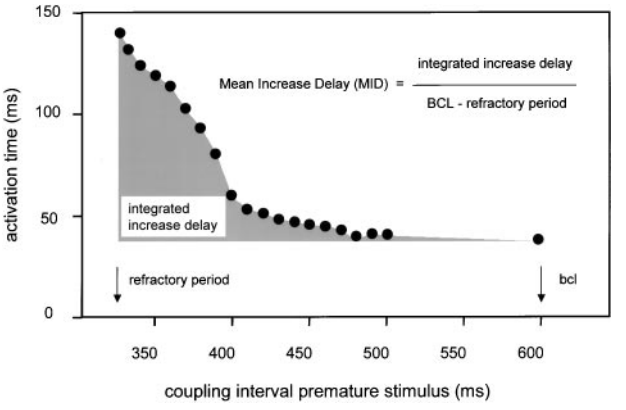

Figure 1. Conduction curve illustrating definition of the mean increase of activation delay. Activation time at the recording site is determined during BCL (600 ms) and premature stimulation at coupling intervals of 500 ms, down in steps of 10 ms to the refractory period. The area under the conduction curve, referenced to the delay at BCL (integrated increase delay), divided by the interval between BCL and the refractory period yields the MID.

Statistical Analysis

All values are expressed as mean±SD. Student's *t* test or the Mann-Whitney Rank Sum test was used to detect significant differences ($P<0.05$).

Results

Isolated Hearts

Mapping of electrical activity was performed at 26 epicardial sites in the 8 Langendorff-perfused hearts (1 to 7 recording sites for each heart). For each position of the plaque electrode, 1 to 4 pacing sites were used (60 in total). Recording areas

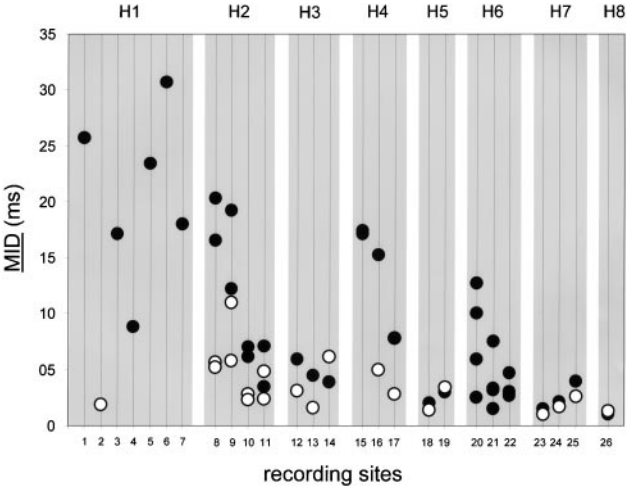

Figure 2. Average value of the MID for all 26 positions (numbers 1 to 26) of the plaque electrode in 8 Langendorff-perfused human hearts (H1 through H8). Multiple open and solid circles (except for H6) along the vertical lines indicate MID values after stimulation from different sites (1 to 4). At open and solid circles, wave front propagation was nearly parallel or perpendicular to fiber direction, respectively.

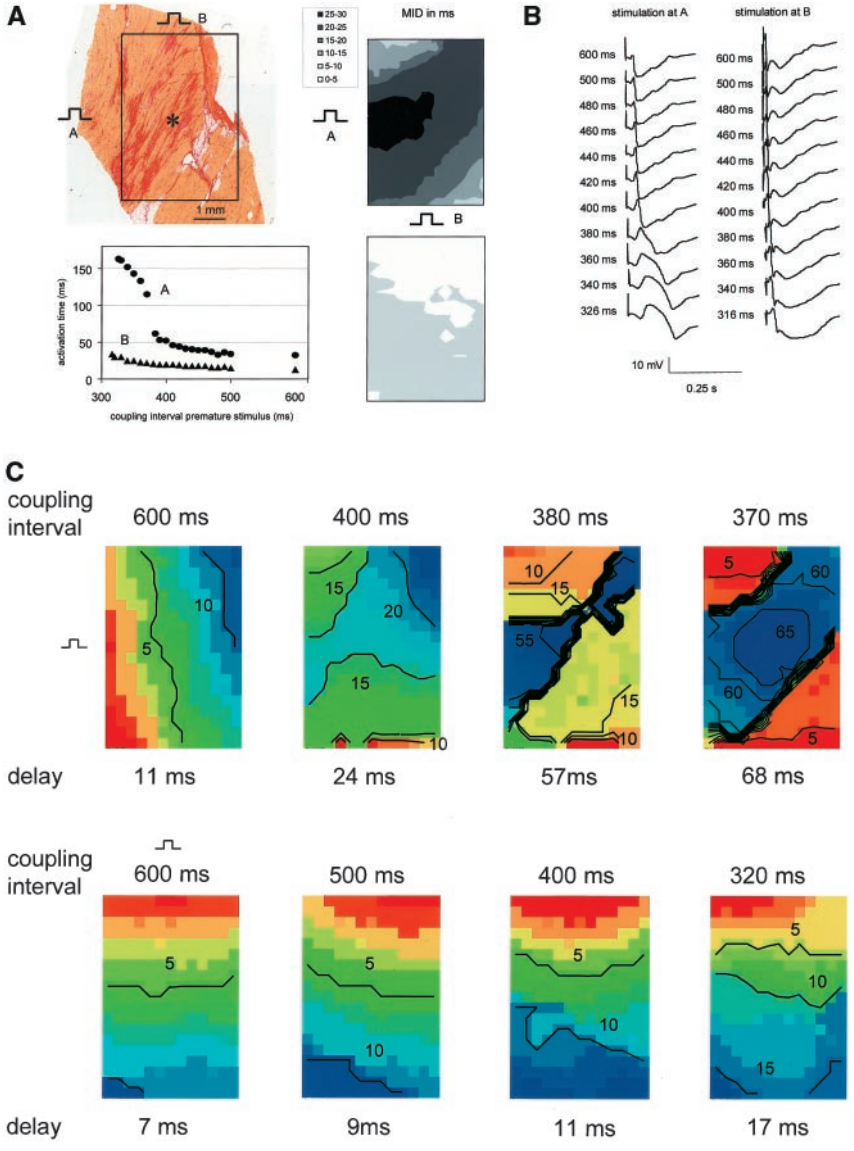

Figure 3. A (Top left), Histological section of the recording area (rectangle) in a heart showing marked fibrosis (red areas). Yellow areas show myocardial tissue. A and B are pacing sites. Bottom left, conduction curves obtained at the asterisk during stimulation at site A and B. Right, MID maps for stimulation at sites A (top) and B (bottom). B, Extracellular electrograms recorded at the asterisk. Numbers are coupling intervals of the premature stimuli. C, Activation maps during stimulation at sites A (top) and B (bottom) during BCL of 600 ms and premature stimuli at coupling intervals from 500 to 320 ms. Numbers beneath maps indicate the time in which the recording area was activated. Activation times range from short (red) to long (indigo). Black lines are isochrones marked with relevant activation times in ms.

were activated within 27.5±12.7 ms during stimulation at BCL. This value increased to 58.5±32.2 ms for activation induced by premature stimuli having a coupling interval 10 ms longer than the refractory period. The mean effective refractory period at the stimulation sites was 346±40 ms.

MID and Fiber Direction

Figure 2 shows the MID for all 26 positions (vertical lines) of the plaque electrode in the 8 Langendorff-perfused hearts. Multiple dots along the vertical lines point to MID values determined at the same recording position of the plaque electrode during pacing at different sites. Open and solid circles are MID values obtained during propagation of wave fronts parallel and perpendicular to the fiber direction (angle between wave front and fiber direction at 0 to 30 or 60 to 90 degrees, respectively).

MID was significantly greater ($P=0.001$, Mann-Whitney test) if pacing resulted in propagation of the electrical impulse perpendicular to the fiber direction (13.1±8.6 ms) instead of propagation parallel to the fibers (4.8±2.8 ms). When MID was <3.5 ms, there was no statistically significant difference for propagation parallel versus perpendicular to the fiber direction ($P=0.15$; paired t test for 6 positions of the multielectrode in 3 hearts).

Figure 3 is an example illustrating the effect of fiber direction on MID in a heart from a patient with coronary artery disease. Histological analysis of the section in Figure 3A revealed 22% fibrosis. MID of the recording area was 20 ms when stimulation was applied at site A. Pacing at this site resulted in activation waves propagating nearly perpendicular to the fiber direction. MID of conduction curve A (lower left panel) determined at the central electrode terminal (*) was 25 ms. The MID map in the upper right panel shows that MID values are high (dark) in the area where major fibrosis is present; MID values decrease toward the upper and lower borders of the recording area. When stimulation was applied at site B, wave fronts propagated almost parallel to the fiber direction and a close to normal conduction curve ensued at the central recording site (curve B indicated by triangles; MID=5 ms). The MID map in the lower right panel shows

that MID values within the recording area are much smaller for propagation parallel to the fiber direction compared with values during propagation perpendicular to it. The extracellular electrograms recorded in the center (Figure 3B) illustrate the progressive increase in conduction delay during premature stimulation at site A.

Activation maps (Figure 3C) during baseline stimulation at site A (upper left map) revealed widely separated isochronal lines, compatible with continuous conduction.

After premature stimulation, however, conduction became irregular with functional lines of conduction block at decreasing coupling intervals. Delay of activation within the recording area increased from 11 to 68 ms. Activation patterns resulting from stimulation at site B (lower maps) showed no irregularities after premature stimuli, and only a marginal increase of conduction delay was observed (from 7 to 17 ms).

MID and Fibrosis

The mean density of fibrosis in the recording areas ranged from 7% to 43% (mean, 18±10%). Three types of fibrosis with regard to architecture were distinguished. These included patchy (patchy fibrosis with long, compact groups of strands; section in Figure 3A), diffuse (more or less diffusely distributed fibrosis with short strands; section in Figure 4), and stringy (homogenously distributed fibrosis with long, single strands; section in Figure 6A). Sometimes local, compact areas of fibrosis were present with stringy fibrosis.

Although the density of fibrosis did not correlate with MID, the architecture of fibrosis played a major role. This is illustrated by comparing Figures 3 and 4. The upper panel of Figure 4 shows a recording area with diffuse fibrosis and a mean density of 33%, which is similar to the section in Figure 3A (mean density, 22%). In contrast to Figure 3A, the MID maps in Figure 4 reveal low values throughout the area for both conduction parallel (upper panel) and perpendicular (lower panel) to the fiber direction. Figure 5 is a scatter plot of MID (propagation perpendicular to fiber direction) and density of fibrosis that illustrates that high values of MID are usually associated with patchy or stringy fibrosis. In areas with diffuse fibrosis, low values of MID are found, even at high densities of fibrosis.

MIDs for patchy and diffuse fibrosis differed significantly (18.4 ms and 5.6 ms for propagation perpendicular to fiber direction, respectively), although the mean density of fibrosis was similar (Table). Conduction velocity during BCL hardly differed for patchy and diffuse fibrosis. Only after premature stimulation is the reduction in conduction velocity perpendicular to fiber direction much greater in patchy than in diffuse fibrosis.

Inexcitable Barriers in Superfused Human Preparations

In 2 superfused preparations with stringy fibrosis, a localized, distinct band of dense fibrosis was present. The effect of this fibrotic band on conduction curves is illustrated in Figure 6. Activation maps during baseline and premature stimulation are shown in Figures 6C and 6D. Figure 6A shows the histology of the recording area (rectangle). Conduction

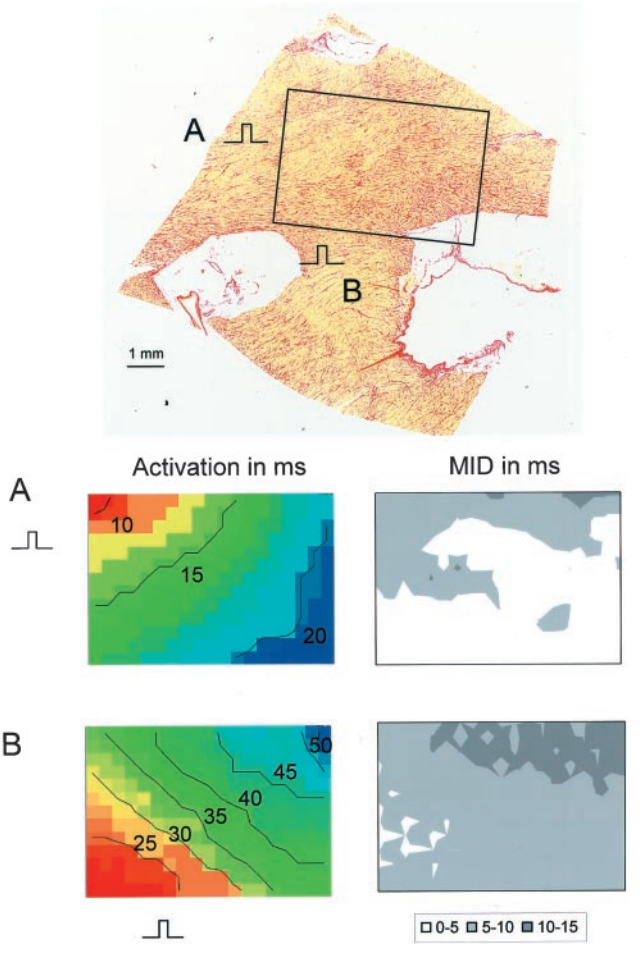

Figure 4. Top, Histological section of the recording area (rectangle) in a heart with dilated cardiomyopathy showing diffuse fibrosis (density, 33%). Red areas mark fibrosis; yellow areas, myocardial tissue. A and B are pacing sites. Bottom left, Activation maps for pacing at BCL of 600 ms at sites A and B. See Figure 3C for color code. Bottom right, corresponding MID maps.

curves, together with the MIDs at sites a through c in the section, are illustrated in Figure 6B. Although the fibrotic barrier (bold arrow) only marginally affected the activation pattern during BCL (Figure 6C), the situation was quite different after premature stimulation (Figure 6D). The lower

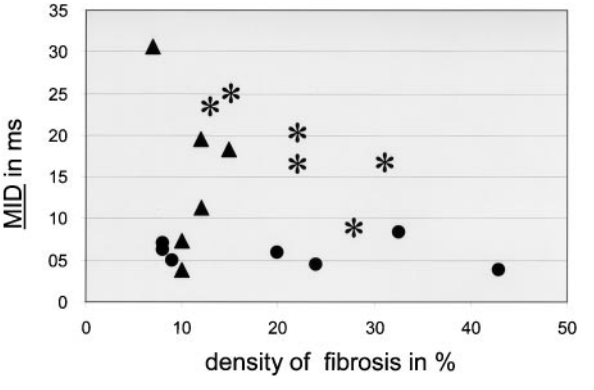

Figure 5. Scatterplot of density of fibrosis and MID for different types of fibrosis (patchy, *; stringy, ▲; or diffuse, ●).

Conduction Velocity During BCL and After Premature Stimulation for Different Types of Fibrosis

Fibrosis	MID, ms†	% Fibrosis	CV⊥BCL, m/s†	CV⊥Extra, m/s*	CV∥BCL, m/s	CV∥Extra, m/s
Diffuse (n=7)	5.6±1.2	20.7±13.7	0.24±0.04	0.17±0.06	0.58±0.15	0.41±0.22
Patchy (n=6)	18.4±5.8	21.8±13.8	0.28±0.07	0.05±0.01	0.57±0.13	0.31±0.12
Stringy (n=6)	14.9±5.8	11.8±2.7	0.39±0.13	0.11±0.09	0.53±0.19	0.27±0.06

Values are mean±SD. CV⊥BCL and CV∥BCL indicate conduction velocity perpendicular (⊥) and parallel (∥) to fiber direction during basic cycle length; CV⊥Extra and CV∥Extra, conduction velocity perpendicular and parallel to fiber direction after a premature stimulus 10 ms longer than the refractory period.

Significant for pairwise comparison of *diffuse vs patchy or †diffuse vs stringy.

left quadrant of the recording area reveals the highest values of MID (7.1 ms at site a). In contrast, MID at sites b and c, where spread of activation remained similar after premature stimulation, was 3.2 ms (site b) and 2 ms (site c).

Discussion

Results show that in chronically diseased human myocardium, a progressive increase of conduction delay during premature stimulation arises in areas with patchy fibrosis having long, compact groups of strands. Delay strongly depends on the direction of wave front propagation with respect to fiber direction; the effect during propagation perpendicular to the fiber direction is large compared with that found during parallel propagation. Diffusely distributed fibrosis with short strands only marginally affected conduction delay, even at high densities of fibrosis.

Discontinuities

Surviving myocardium in infarcted and cardiomyopathic hearts often exhibits near-normal intracellular electrophysiological characteristics, although extracellular electrograms are often fractionated.[11–14] Conduction in these hearts is often affected by fibrosis, which forms isolating barriers and discontinuities.

The effect of several types of tissue discontinuities on propagation have been investigated, including (1) inexcitable barriers with a narrow isthmus,[8] (2) inexcitable barriers causing wave fronts to curve,[15] and (3) load mismatch.[7] Data from these studies show that conduction delay at discontinuities is a common denominator. In addition, delay increases with a decrease in the cycle length of activation.[7,8] Similar discontinuities are present in the hearts we studied, and due to the cycle length dependence, they may give rise to a progressive increase of conduction delay and MID.

Architecture of Fibrosis

Results revealed that the architecture of fibrosis played a major role in determining the progressive increase of conduction delay at incremental shortening of the coupling interval of the premature stimulus. The effect of long fibrotic strands on conduction and MID was much greater than that with diffuse fibrosis with short strands. This is compatible with observations made by Pertsov[16] in a model mimicking myocardial texture. This model showed that a decrease in the number of lateral connections increased anisotropy and amplified the effects of discontinuous conduction. However, there was no direct relation between discontinuous propagation and anisotropy. Discontinuous propagation vanished when the texture size (equivalent to the length of the fibrotic strands) was scaled down sufficiently, whereas anisotropy in conduction velocities was not affected by scaling the texture size. In the hearts we studied, fibrotic strands in areas with

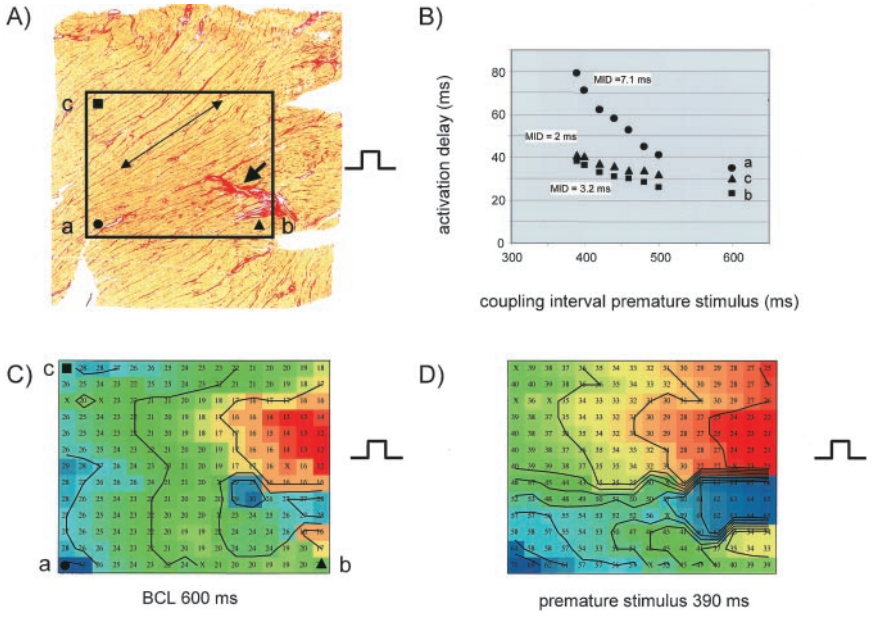

Figure 6. A, Histological section of the recording area (rectangle) of a superfused epicardial preparation from an explanted human heart with dilated cardiomyopathy. Red areas point to fibrosis; yellow areas, myocardial tissue. The bold arrow marks a broad zone of dense, fibrosis, and the long arrow indicates fiber direction. B, Conduction curves obtained during stimulation at the site indicated by the stimulus marker. Symbols match those at recording sites a, b, and c indicated in A. C and D, Activation maps at BCL of 600 ms and after premature stimulation. See Figure 3C for color code.

diffuse fibrosis were apparently too short to cause discontinuous conduction. In addition, the effect of uniform anisotropy on MID was low.

Fibrosis and Abnormal Conduction

Fibrotic tissue has been shown to decrease the safety factor for impulse propagation, leading to conduction block and the development of reentry.[17] Other investigators have shown that sites of increased fibrosis or scar tissue are often involved in the generation of unidirectional conduction block, leading to wave break and reentry.[18] Conduction abnormalities related to fibrotic tissue infiltration have been observed in ventricular tissue with infarction and cardiomyopathy, as well as in atrial myocardium of animal models of atrial fibrillation. Li et al[19] showed that extensive interstitial fibrosis promoted atrial fibrillation in a dog model of heart failure. These data are compatible with our observation that interstitial fibrosis leads to discontinuous propagation and the spatial dispersion of conduction, creating a potential substrate for reentry.

Activation Delay Caused by Inexcitable Barriers

Figure 6 indicates that an inexcitable barrier may lead to an increase of activation delay due to the following factors: (1) increase of the path length (although activation toward recording site a in Figure 6 reaches this site via a route running inferiorly as well as superiorly of the fibrotic barrier during BCL, the route lies superiorly of the barrier and is longer after premature stimulation); (2) change from longitudinal to transverse conduction (during stimulation at BCL, activation runs mainly parallel to the fiber direction; however, after premature stimulation, the activation front runs perpendicular to the fiber direction after passing the barrier to reach site a, which increases delay); (3) wave front curvature (at the distal end of the barrier, the wave front curves, resulting in an increase of activation delay[8]); and/or (4) reduced conduction velocity (conduction velocity decreases in the area superiorly of the barrier from 0.5 m/s during baseline to 0.32 m/s after a premature stimulus of 390 ms).

Reduced Sodium Current

Pu and Boyden[20] observed reduced excitability in the epicardial border zone of the infarcted canine heart. Their study showed that in the infarcted myocardium, Na^+ channel expression was suppressed. Measurements were carried out in myocytes derived from the epicardial border zone of canine hearts after 5 days of infarction. Although these hearts were studied at a relatively early stage after the onset of infarction, we cannot completely exclude the possibility that Na^+ current abnormalities may have played a role in our hearts.

Clinical Relevance

Clinical and experimental studies suggest an association between conduction abnormalities or fibrosis and ventricular arrhythmias or sudden death.[4,15,21] Although nonuniform anisotropy in patients with ventricular tachycardia has been shown to be associated with reentry in healed myocardial infarction, it is not known what degree of nonuniformity is required to alter vulnerability to arrhythmias. Our data show that the architecture of fibrosis is more important than its density for generating conduction disturbances. In addition, the course of conduction curves strongly depends on the direction of the wave front, which implies that conduction curves should be critically evaluated when used for risk stratification.

Limitations of the Study

We concentrated on histological characteristics. However, it has been shown that changes in connexin distribution and expression occur in infarcted and hypertrophic myocardium, giving rise to cellular uncoupling.[22] Although computer simulations suggest that a profound reduction in cell-cell coupling is required to affect conduction, the role of changes in connexins with respect to early onset of activation delay in diseased hearts cannot be entirely ruled out.[23]

We determined activation delay from the stimulus, which might have led to a slight overestimation of the MID values.

Recordings in the Langendorff-perfused hearts were not always made at the same site in each heart. Recording positions were chosen in areas without excessive fatty tissue to allow for epicardial recordings. Although recording sites were evenly distributed over the hearts, we cannot rule out the possibility that this selection affected our results.

Acknowledgment

Dr de Groot is supported in part by the Dutch Heart Foundation (grant 2000D020).

References

1. Myerburg RJ, Kessler M, Castellanos A. Sudden cardiac death: epidemiology, transient risk, and intervention assessment. *Ann Intern Med*. 1993; 119:1187–1197.
2. Rosenbaum DS, Albrecht P, Cohen R. Predicting sudden cardiac death from T wave alternans of the surface electrogram: promise and pitfalls. *J Cardiovasc Electrophysiol*. 1996;7:1095–1111.
3. Barr CS, Naas A, Freedman M, et al. QT dispersion and sudden unexpected death in chronic heart failure. *Lancet*. 1994;343:327–329.
4. Saumarez RC, Slade AKB, Grace AA, et al. The significance of paced electrogram fractionation in hypertrophic cardiomyopathy: a prospective study. *Circulation*. 1995;91:2762–2768.
5. Shaw RM, Rudy Y. Electrophysiologic effects of acute myocardial ischemia: a theoretical study of altered cell excitability and action potential duration. *Cardiovasc Res*. 1997;35:256–272.
6. Gettes LS, Cascio WE. Effect of acute ischemia on cardiac electrophysiology. In: Fozzard HA, Jennings RB, Haber E, et al, eds. *The Heart and Cardiovascular System*. New York: Raven Press; 1992:2021–2054.
7. Fast VG, Kléber AG. Cardiac tissue geometry as a determinant of unidirectional conduction block: assessment of microscopic excitation spread by optical mapping in patterned cell cultures and in a computer model. *Cardiovasc Res*. 1995;29:697–707.
8. Cabo C, Pertsov AM, Baxter WT, et al. Wave front curvature as a cause of slow conduction and block in isolated cardiac muscle. *Circ Res*. 1994;75:1014–1028.
9. de Bakker JMT, van Capelle FJL, Janse MJ, et al. Slow conduction in the infarcted human heart: zig-zag course of activation. *Circulation*. 1993; 88:915–926.
10. de Bakker JMT, van Capelle FJL, Janse MJ, et al. Fractionated electrograms in dilated cardiomyopathy: origin and relation to abnormal conduction. *J Am Coll Cardiol*. 1996;27:1071–1078.
11. Ursell PC, Gardner PI, Albala A, et al. Structural and electrophysiological changes in the epicardial border zone of canine myocardial infarcts during infarct healing. *Circ Res*. 1985;56:436–451.
12. Spear JF, Horowitz LN, Hodess AB, et al. Cellular electrophysiology of human myocardial infarction, I: abnormalities of cellular activation. *Circulation*. 1979;59:247–256.

13. de Bakker JMT, van Capelle FJL, Janse MJ, et al. Reentry as a cause of ventricular tachycardia in patients with chronic ischemic heart disease: electrophysiologic and anatomic correlation. *Circulation*. 1988;77: 589–606.
14. Gardner PI, Ursell PC, Fenoglio JJ, et al. Electrophysiologic and anatomic basis for fractionated electrograms recorded from healed myocardial infarcts. *Circulation*. 1985;72:596–611.
15. Davidenko JM, Cabo C, Jalife J. Wave-front curvature leads to slow conduction and block in two-dimensional cardiac muscle. In: Spooner PM, Joyner RW, Jalife J, eds. *Discontinuous Conduction in the Heart*. New York: Futura; 1997:295–319.
16. Pertsov A. Scale of geometric structures responsible for discontinuous propagation in myocardial tissue. In: Spooner PM, Joyner RW, Jalife J, eds. *Discontinuous Conduction in the Heart*. New York: Futura; 1997: 273–293.
17. Spach MS, Miller WT Jr, Dolber PC, et al. The functional role of structural complexities in the propagation of depolarization in the atrium of the dog: cardiac conduction disturbances due to discontinuities of effective axial resistivity. *Circ Res*. 1982;50:175–191.
18. Wu TJ, Ong JJC, Hwang C, et al. The characteristics of wave fronts during ventricular fibrillation in human hearts with dilated cardiomyopathy: role of increased fibrosis in the generation of reentry. *J Am Coll Cardiol*. 1998;32:187–196.
19. Li D, Fareh S, Ki Leung T, et al. Promotion of atrial fibrillation by heart failure in dogs; atrial remodeling of a different sort. *Circulation*. 1999; 100:87–95.
20. Pu J, Boyden PA. Alterations of Na^+ currents in myocytes from epicardial border zone of the infarcted heart: a possible ionic mechanism for reduced excitability and postrepolarization refractoriness. *Circ Res*. 1997;81: 110–119.
21. Anderson KP, Walker R, Urie P, et al. Myocardial electrical propagation in patients with idiopathic dilated cardiomyopathy. *J Clin Invest*. 1993; 92:122–140.
22. Peters NS, Green CR, Poole-Wilson PA, et al. Reduced content of connexin43 gap junctions in ventricular myocardium from hypertrophied and ischemic human hearts. *Circulation*. 1993;88:864–875.
23. Jongsma HJ, Wilders R. Gap junctions in cardiovascular disease. *Circ Res*. 2000;86:1193–1197.

Activation Delay After Premature Stimulation in Chronically Diseased Human Myocardium Relates to the Architecture of Interstitial Fibrosis

Tokuhiro Kawara, Richard Derksen, Joris R. de Groot, Ruben Coronel, Sara Tasseron, André C. Linnenbank, Richard N.W. Hauer, Hans Kirkels, Michiel J. Janse and Jacques M.T. de Bakker

Circulation. 2001;104:3069-3075
doi: 10.1161/hc5001.100833
Circulation is published by the American Heart Association, 7272 Greenville Avenue, Dallas, TX 75231

Print ISSN: 0009-7322. Online ISSN: 1524-4539